Individual tree crown detection and delineation across a woodland using leaf-on and leaf-off imagery from a UAV consumer-grade camera

Elias Fernando Berra[a,b,*]

[a]Newcastle University, Geospatial Engineering Group, Newcastle upon Tyne, United Kingdom
[b]Federal University of Rio Grande do Sul, State Research Center for Remote Sensing and Meteorology, Porto Alegre, Brazil

Abstract. Extraction of information about individual trees using remotely sensed data is essential to supporting ecological and commercial applications in forest environments. Data acquired by consumer-grade cameras onboard unmanned aerial vehicles (UAV) offer an affordable option of high-spatial resolution imagery that can be used to extract forest structural information at a tree level. The aim of this work is to investigate the potential and accuracy of UAV time-series data to automatically detect and delineate tree crowns across an entire woodland. The workflow (presented in a step-by-step manner) involves the construction of a canopy height model (CHM) based on digital elevation models derived from the UAV photogrammetric point clouds. A watershed-based approach is modified to automatically detect and delineate the tree crowns, based on the CHM and the brightness information from the UAV orthomosaics. The accuracy of the proposed method was evaluated by comparing its results against manually delineated tree crowns. The results show an overall accuracy of 63%, where conifer species were more accurately delineated (up to 80%), while broadleaf species returned lower accuracies (<50%). Continued research is necessary to improve the confidence of automated individual tree crown detection and delineation, especially over complex forest structures. © *2020 Society of Photo-Optical Instrumentation Engineers (SPIE)* [DOI: 10.1117/1.JRS.14.034501]

Keywords: crown delineation; drone; forest inventory; watershed algorithm; phenology; consumer off-the-shelf.

Paper 200086 received Jan. 29, 2020; accepted for publication Jun. 25, 2020; published online Jul. 3, 2020.

1 Introduction

Individual tree crowns, which are associated with the location and size of individual trees, can provide important structural information of a forest ecosystem. The automatic and accurate detection of individual tree crowns has many ecological and commercial applications, including forest planning,[1] optimizing orchard management,[2] evaluating tree growth dynamics,[3] improving tree species classification,[4,5] estimating diameter at breast height and above-ground biomass,[6] and tree cover estimation.[7] Remote sensing data and techniques have been increasingly used to automatically detect and count tree crowns in substitution and/or in complement to traditional forest inventories, which are time-consuming and expensive.[5,8] However, the accurate identification of individual trees across diverse forest ecosystems in remote sensing data using automated methods is still not an easy task.[9] Therefore, obtaining automatic identification of tree crowns, their locations, and counts from remotely detected data is a useful and challenging task.[10]

Aerial mapping of three-dimensional (3-D) forest structure has been largely undertaken with the aid of airborne laser scanning (ALS) technology,[11–13] and more recently, unmanned aerial vehicle (UAV) imagery has emerged as a feasible and cost-effective local scale option for this purpose.[14–20] This is possible due to the advances in structure-from-motion and multiview stereo techniques, which have allowed digital terrain models (DTMs) and digital surface models

*Address all correspondence to Elias Fernando Berra, E-mail: eliasberra@gmail.com

(DSMs) to be generated out of 3-D photogrammetric point clouds.[15] In a forest environment, the underlying ground topography (DTM) can be reconstructed based on points classified/selected as ground.[14] A canopy height model (CHM) can, therefore, be obtained by subtracting these two elevation models and forest attributes (e.g., total tree height and tree crown area) can potentially be derived from the CHM at an individual tree level, similarly to ALS data.[16]

There are many approaches available to detect and delineate tree crowns from a CHM, with no single method performing best for all applications.[8,21] The accuracy of single-tree-level attributes estimation can be affected by the delineation method and data chosen but also, it can be highly dependent on the forest structure under investigation.[10,12,22] Individual tree-level prediction accuracies of complex canopy structures (e.g., old broadleaf forest and uneven-aged trees) are usually lower than those found in simpler and more homogeneous structures (e.g., conifer-dominated forests and same-age plots).[23,24] Therefore, there is a need for continued research in either new algorithms or new remote sensing datasets to improve individual tree crown delineation.

Several studies have tested the potential of UAV data acquired from low-cost red–green–blue (RGB) digital cameras for individual tree parameters detection,[14,16–19,25–29] but they present a combination of methods, forest types, and estimated metrics that are mostly different from the work described here, including (i) focus on a single date acquisition,[14,16–19,25,26,29] (ii) monospecific forest plantations or crop trees,[16,25,26,28] (iii) using the spectral information [or image digital number (DN) values] alone,[26] and (iv) using the photogrammetric point clouds-derived products (e.g., CHM) alone.[14,16,25,28,30] Comparatively, fewer studies used both the photogrammetric point clouds and the spectral data, but the spectral information was used to classify tree species[15,19] and to predict forest biophysical parameters,[17] not being incorporated into the individual tree detection algorithm. In one study, however, Yancho et al.[29] combined point clouds with spectral information for individual tree crown detection but, unlike the raster-based methodology proposed here, the authors worked in the point-level domain to form subcrown clustering. Nuijten et al.[30] and Yancho et al.[29] suggested that future research should explore different ways to incorporate the spectral information into individual tree detection methods, across a diversity of forest environments.

The aim of this work is to investigate the potential and accuracy of leaf-on and leaf-off imagery acquired by a consumer-grade RGB camera onboard a UAV to automatically detect and delineate tree crowns across a heterogeneous woodland with conifer and broadleaved species. More specifically, this paper assesses the effect of combining photogrammetric point clouds-derived CHM and orthomosaic brightness values (raster datasets) to detect and delineate individual tree crowns (while retrieving associated tree heights and crown diameters), adding further understanding on how spectral information may be used in individual tree detection. The work uses UAV data acquired on two dates (leaf-on and leaf-off) to better reconstruct the DTM and the DSM, without intending to quantify errors associated with mapping crowns over time, as this is already done elsewhere.[30] While the accuracy of the delineated crows was evaluated by comparing its results against manually delineated tree crowns, the height and crown diameter were validated against ground measurements. In addition, the chosen methodology is described in a detailed, step-by-step manner (almost as a guide) to facilitate reproducibility and adoption by the community. Finally, the potential and uncertainties of the proposed method are discussed for applications in forest phenology studies.

2 Methodology

2.1 *Study Area and UAV Data Collection*

The study area was previously described by Berra et al.[31] Briefly, the study area consists of 15 ha of mixed deciduous and evergreen (conifer and broadleaf) woodland in the northeast of England (Fig. 1). The terrain within the woods has relatively flat topography with an altitude of ~75 m above sea level. A temperate climate is observed with a mean annual temperature of 8.3°C.[32] Ground and UAV data were collected during the spring season of 2015, as part of an intensive field campaign to characterize the spring phenology [e.g., day of year (DOY) of appearance of

Fig. 1 Orthomosaic made of UAV images (visible camera) acquired on April 21, 2015. Ground validation data were acquired in six different plots (each containing 20 trees). The woodland was classified in four different land cover types. The Great Britain national outline is a product of ©Crown copyright and database rights 2016 Ordnance Survey.

first leaves] of the study area.[31] Section 4.1 discusses the potential of the proposed methodology for phenology studies.

Six plots were installed to sample 20 individuals[33] from the main tree species within this woodland (locations are shown in Fig. 1). The plots' names and respective tree species are as follows.

1. Larch: European larch (*Larix decidua*),
2. Sycamore: Sycamore (*Acer pseudoplatanus* L.),
3. Oak: Sessile oak (*Quercus petraea*),
4. Sitka spruce: Sitka spruce (*Picea sitchensis*),
5. Norway spruce: Norway spruce (*Picea abies*), and
6. Mix: English oak (*Quercus robur*) and sycamore.

Geographical coordinates of the 120 trees were surveyed with total station and Global Navigation Satellite System (GNSS). Tree height was measured using a vertex hypsometer (Vertex IV) and transponder (Transponder T3) (Haglof Sweden AB, Langsele, Sweden). The following average and variability in tree height was observed within each plot: Larch (21.3 ± 2.4 m), Sycamore (20.5 ± 1.2 m), Oak (19.6 ± 3.1 m), Sitka spruce (19.1 ± 0.8), Norway spruce (15.8 ± 0.9 m), and Mix (18.9 ± 4.5 m).

The collection, processing, calibration, and validation of the series of UAV data used in this paper are described in detail by Berra et al.[31,34] Briefly, the study area was flown by a fixed-wing UAV (Quest300 and QPOD—QuestUAV Ltd., Amble, UK) equipped with one gimballed Panasonic DMC-LX5 digital camera (Panasonic UK Ltd., Bracknell, Berkshire, UK). The camera has 5.1-mm nominal focal length, 3648×2736 pixels (effective pixels 10 megapixels), CCD sensor type with a sensor size of $1/1.63$ in. and records the visible light in the RGB channels (Table 1). The Panasonic's relative spectral response functions can be seen in Ref. 34.

All UAV images were captured on manual settings (ISO-100, shutter speed $1/800$ s, aperture $f/2$, and focus to infinity) and saved in RAW format. The RAW files were individually converted to dark- and vignetting-corrected linear TIFF images (i.e., RGB image).[31,34] The corrected TIFF images were thereafter mosaicked using the software Agisoft PhotoScan v.2 (Agisoft LLC, St. Petersburg, Russia). Orthomosaics were created following recommended settings,[35] but with a key modification: the orthomosaic was constructed with blending mode deactivated to preserve the original (corrected) DN values. While surface reflectance was retrieved from the orthomosaic DNs by Berra et al.,[31,34] this work uses only the orthomosaic DN values (referred to as brightness values in this paper) without any further correction.

Table 1 Spectral settings of the RGB Panasonic camera. FWHM: full width at half maximum.

Band	Band width (nm)	FWHM wavelength (nm)		Center wavelength (nm)
		Lower	Upper	
Blue	87	426	512	469
Green	121	473	595	534
Red	76	579	655	617

Table 2 Characteristics of the UAV imagery acquisition, derived products and from which date each product was extracted.

Acquisition date	Season	Images	Flight height (m)	Elevation model	Points per m^2	RGB brightness
March 18, 2015	Winter (leaf-off)	499	122	DTM	122	No
August 6, 2015	Summer (leaf-on)	429	122	DSM	110	Yes

The orthomosaics (spatial resolution of 10 cm and geolocation accuracy of ± 11 cm) and associated point clouds were generated for two dates (Table 2): March 18, 2015 (leaf-off) and August 6, 2015 (leaf-on). This was done to take advantage of the: (i) leaf-off phase of deciduous species as to detect a higher density of ground points for later DTM calculations and (ii) leaf-on phase to produce a higher density of tree canopy points for later DSM reconstruction. More details of the orthomosaic and digital elevation models generation are provided in the following section.

2.2 *Automatic Tree Crown Delineation Based on CHM*

In this paper, the automatic tree crown delineation across the entire study area was achieved using a watershed-based approach, as proposed by Panagiotidis et al.,[14] who used very high-resolution UAV imagery, similar to the imagery available in this study, as input data to delineate tree crowns. Because watershed algorithm is easy to be implemented and improved, well developed,[8,10] and is commonly available in geographic information system (GIS) software, watershed is frequently used to perform crown delineation from a CHM.[1,2,10,14,22,36–38] Panagiotidis et al.'s[14] original workflow, which used only 3-D data, was modified in this study to also include the orthomosaic's RGB brightness information in the processing chain (Fig. 2) to test whether this would increase the delineation accuracy.

UAV images from two dates were used as input to generate a CHM (Table 2). On each date, the study area was flown twice to have a higher rate of image overlapping, which in turn can produce a denser point cloud, resulting in a more detailed 3-D model and potentially minimizing occlusion problems.[15,19] The DTM was derived from a UAV acquisition date corresponding to deciduous leaf-off phase (DOY 77, March 18, 2015) to have a higher density of points representing the ground, at least over deciduous covers. UAV images acquired during a deciduous leaf-on phase were used to derive a DSM (DOY 218, August 6, 2015) as the canopy foliage was fully developed on this date.

After image alignment within PhotoScan (498 out of 499 aligned on DOY 77 and 429 out of 429 on DOY 218), the resulting sparse point cloud was georeferenced using 13 ground control points (GCPs). Thereafter, the camera parameters were optimized and a denser point cloud was generated using a high-quality reconstruction setting within PhotoScan.[35] From the dense point cloud of DOY 77 (122 points/m^2), an automatic classification (within PhotoScan) detected points associated with the ground. This classification is based on three user-defined parameters

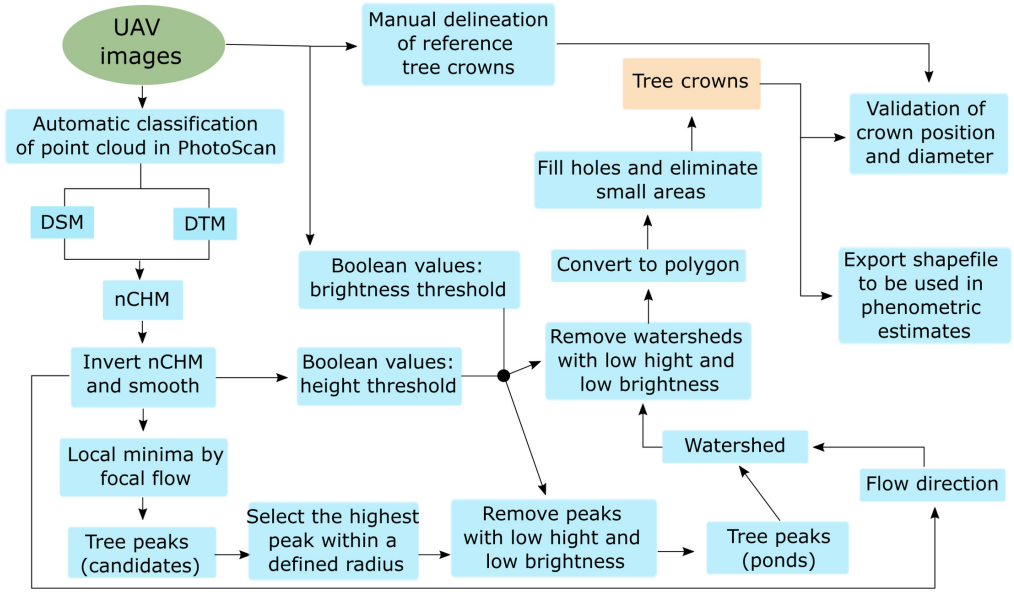

Fig. 2 Flowchart of the UAV data processing for automatic delineation of tree crowns. Modified from Ref. 14.

(maximum angle = 15 deg, maximum distance = 1 m, and cell size = 150 m), values which were determined based on a trial and error approach. The point cloud is first divided into the chosen cell size [150 m represents the approximate size of the largest evergreen stand (closed canopy; Sitka spruce in Fig. 1), where fewer ground points are likely to be present], and the lowest point within each cell is detected. An initial terrain model is triangulated from these points. Then, the remaining points are iteratively checked and added to the ground class if they satisfy the specified angle and distance (in relation to the terrain model).[35,39] A DTM is then build based on the selected ground points employing the "enabled (default)" interpolation option within PhotoScan. The DSM was constructed using the entire dense point cloud from DOY 218 (110 points/m^2), using the same interpolation option. The DSM and DTM were exported as raster files (10-cm spatial resolution) to be used as input in ArcGIS 10.3.1 (ESRI©).

ArcGIS's model builder was used to automate the tree crown delineation (Fig. 2). First, a normalized CHM (nCHM) was calculated by subtracting the DTM from the DSM. The nCHM was then inverted to allow the inverse watershed segmentation method[2,36] to be applied, whereby each segment is considered as an individual hydrologic drainage basin. In addition to the inverted surface, a watershed approach also needs markers or "ponds" (tree peaks in this case), which was achieved using the following three steps.

1. Determination of local minima by focal flow statistics. This step returned many tree peaks, not only over crown areas but also on the ground, so cleaning and selection were applied.
2. Selection of the highest peak within a defined circular radius (focal statistics). The optimal radius was determined per woodland type based on a trial and error approach (Larch = 2 m, Sycamore = 2.2 m, Oak = 2.7 m, Sitka spruce = 1.5 m, Norway spruce = 0.9 m, and Mix = 2.4 m).
3. Removal of peaks by testing two methods:

    1. "CHM only," using only the CHM data (similar to Ref. 14): Removal of peaks with low height (below the average CHM value of a 5×5 m window).
    2. "CHM + brightness," by combining CHM and the orthomosaic's brightness values: Removal of peaks with low height (as above) and low brightness. This later step was added into Panagiotidis et al.'s14 workflow by defining a brightness threshold (either 20% or 30% percentiles, dependent on woodland type) from the green band of the orthomosaic of DOY 218. The green band was chosen as it has

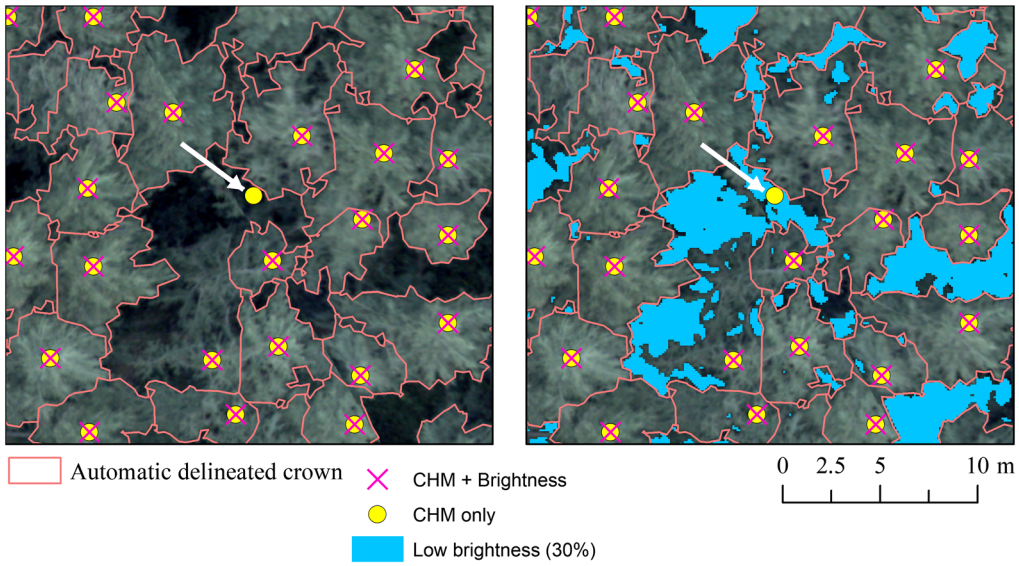

Fig. 3 Example of tree crowns and peaks extracted over the Larch dominated area. Tree peaks extracted by both the CHM only (yellow circle) and the CHM + brightness (pink X) methods are shown. The white arrow indicates a tree peak that was incorrectly detected when using the CHM data alone. On the other hand, by incorporating the orthomosaic values into the workflow (CHM + brightness), the candidate tree peak was excluded (filtered out) as it falls into a low brightness area.

the highest signal-to-noise ratio (Table 1). This was undertaken to eliminate peaks located either on the edge of crowns or very close to the crown (peaks which were not eliminated by the height threshold alone), as shown in Fig. 3. Low brightness areas are expected to detect canopy shadows which are related to canopy gaps among the tree crowns (Fig. 3); vegetation indices (instead of individual bands) were not used as they tend to minimize shadowing effects,[40] outcome which was not desired for this study.

Watershed segmentation was then applied using both the selected tree peaks (imitating ponds) and nCHM-derived flow direction as inputs (Fig. 2). The later raster was created using the "flow direction" tool within ArcMap, where each output cell represents the direction of flow from the elevation surface (nCHM). Since the segmentation results in a continuous raster, segments falling into areas of either low height (CHM only method) or low brightness and low brightness (CHM + brightness method) were removed using the same above-mentioned thresholds.

Finally, the resulting watersheds were converted to polygons. Any hole inside a polygon was filled and polygons with small areas (1 to 3 m^2, dependent on woodland type as shown in Fig. 2) were either merged with adjacent ones or eliminated. The remaining polygons represent the tree crowns (as shown in Fig. 6) and they were exported as a shapefile to allow for accuracy checks across the whole study area.

2.3 *Automatic Tree Crown Delineation: Accuracy Assessment*

The validation/reference data consisted of manually delineated crowns, which is a common approach when high- or very high-resolution imagery is available.[21,22,41] Considering the very high-spatial resolution of the UAV orthomosaics (10 cm), tree crowns were extracted by a manual delineation approach in ArcGIS. First, a point dataset containing the location and identification of each sampled tree (surveyed in the field) was overlain on the UAV orthomosaics. Each crown boundary was thereafter drawn based on leaf-on orthomosaics, but both orthomosaics (Table 2) were used to aid the image interpretation, allowing individual crowns to be resolved with confidence. In addition to the 20 trees within each plot (Fig. 1), 20 more tree crowns (surrounding

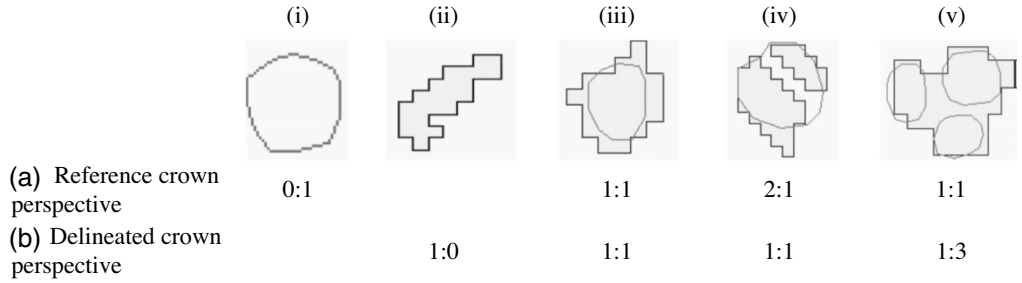

Fig. 4 Detection scenarios from (a) reference and (b) crown perspectives with reference crowns shown as circular polygons and delineated crowns as filled polygons (Adapted from Ref. 22). An interpretation of these five cases (i)–(v) is given in Table 3.

these plots) were manually delineated on the UAV orthomosaics, resulting in 40 crowns per woodland type (Larch, Sycamore, Oak, Sitka spruce, Norway spruce, and Mix), increasing the statistical representativeness.

The watershed-derived tree crowns were quantitatively evaluated at both plot and individual tree level, following the method proposed in Ref. 22. Plot-level assessment consisted of quantifying the tree count errors, i.e., comparing the crown count estimation against the number of reference crowns. However, this analysis does not quantify wrongly/correctly delineated crowns, and Ke and Quackenbush[22] proposed a confusion table to evaluate individual tree-level accuracy from both a reference crown and delineated crown perspective. The method is shown in Fig. 4 with an interpretation provided in Table 3. In summary, the approach quantifies correctly detected tree crowns and errors due to omission, commission, undersegmentation, and oversegmentation.

The results from this confusion matrix are thereafter translated in terms of producer's accuracy (PA) and user's accuracy (UA). PA calculates the probability of a reference tree being correctly delineated [Eq. (1)] and UA represents the probability that a delineated tree will correctly represent a reference tree.[22]

$$\mathrm{PA} = \frac{N_p}{N_r}, \tag{1}$$

$$\mathrm{UA} = \frac{N_p}{N_d}, \tag{2}$$

where N_p is the number of correctly delineated trees, N_r is the number of reference trees, and N_d is the number of delineated trees.

Table 3 Interpretation of the detection scenarios as shown in Fig. 4. Adapted from Ref. 22.

Case	Interpretation
i	Simple omission (0 delineated:1 reference).
ii	Simple commission (1 delineated:0 reference).
iii	Perfect match, i.e., correctly delineated tree (1 delineated:1 reference) in both perspectives.
iv	Commission from oversegmentation. One reference crown is delineated as two crowns, so a "2 delineated:1 reference" ratio from a reference perspective. However, from the delineated crown perspective, each delineated crown sees only one reference crown (1 delineated:1 reference).
v	Omission due to undersegmentation. A group of reference trees is delineated as a single one, resulting in a "1 delineated:3 reference" ratio under the delineated perspective. From a reference crown perspective, however, each reference tree sees only one delineated polygon, so the "1 delineated:1 reference" ratio.

To quantify the effect of adding the orthomosaic brightness values into the original workflow that used only CHM data, the above-mentioned accuracy checks were carried out for both methods: CHM only and CHM + brightness. Accuracy checks for crown diameter and tree height estimates were performed only for the data coming from the method with the least uncertainties.

A final accuracy assessment (for the crown delineation) was undertaken by comparing the delineated crown diameter against the reference diameters, but considering only the correctly delineated tree crowns [case (iii), Fig. 4]. This involved calculation of mean error, absolute error, and RMSE values.

Tree heights derived from the CHM ("tree peaks," as shown in Fig. 2) were linearly regressed against observed tree heights (hypsometer) to quantify the accuracy of the UAV-derived CHM. An intersection test selected the observed versus estimated pairs of data; if the geolocation of an observed height (point) intersects an automatic delineated crown (polygon), then the observed tree height value is associated with the polygon's tree peak value.

Lastly, it was tested whether decreasing image resolution would affect the tree crown delineation error. The spatial resolution of the UAV-derived CHM and orthomosaics were degraded in a 10-cm step up to 50 cm (i.e., 10–20–30–40–50 cm). The PA [Eq. (1)] and UA [Eq. (2)] of tree crown delineated at each of these five spatial scales were compared across the six different test sites.

3 Results

3.1 *Accuracy of the Automatic Tree Crown Delineation*

For the CHM + brightness method, no difference was detected between the number of observed and detected trees in the Larch and Mix plots, while an underestimation of the number of trees was observed for Sycamore, Sitka spruce, and Norway spruce, contrary to overestimation for the Oak plot (Table 4). On the other hand, the CHM only method detected, on average, 5% more trees (Table 4). However, this tree counting does not provide the proportion of correctly delineated trees, information that is given by the reference/crown perspective confusion matrix (Tables 5 and 6).

Considering the CHM + brightness method, an overall accuracy of 63% was detected across all woodland types, as given by the PA and UA (Table 5). Conifer species were more accurately delineated with PA ranging from 73% to 80% (UA from 78% to 82%), while broadleaf species achieved lower PAs (43% to 57%, with UA from 43% to 63%). Only one tree (out of 240) was omitted and no simple commission errors were observed. Oversegmentation affected mainly the

Table 4 Tree count estimation error at plot level, comparing results achieved using the CHM only versus CHM + brightness methods. Every automatically delineated crown (estimated) represents one tree.

		CHM + brightness		CHM only	
Plot	Reference	Estimated	Difference (%)	Estimated	Difference (%)
Larch	40	40	0	41	3
Sycamore	40	35	−13	38	−5
Oak	41	51	24	56	37
Sitka spruce	40	39	−3	44	10
Norway spruce	40	36	−10	32	−20
Mix	40	40	0	42	5
Total	241	241	0	253	5

Table 5 Accuracy assessment of automatically delineated tree crowns for CHM + brightness. The column 1:1 shows the correctly delineated trees or perfect matches. About 40 reference trees were sampled in each plot, totaling 240 reference trees.

	Reference crown perspective				Delineated crown perspective						
Plot	0:1	1:1	2:1	3:1	1:0	1:1	1:2	1:3	1:1	PA[a] (%)	UA[b] (%)
A	0	34	6	0	0	39	1	0	31	78	78
B	0	32	8	0	0	29	6	0	23	57	66
C	1	29	10	1	0	44	5	2	21	51	41
D	0	36	4	0	0	35	3	1	32	80	82
E	0	35	5	0	0	33	3	0	29	73	81
F	0	26	12	2	0	33	5	2	17	43	43
All	1	192	45	3	0	213	23	5	153	63	63

[a]Producer's accuracy.
[b]User's accuracy; A = Larch; B = Sycamore; C = Oak; D = Sitka spruce; E = Norway spruce; F = Mix. A, D, and E are conifers; the others are broadleaf species.

Table 6 Accuracy assessment of automatically delineated tree crowns for CHM only. The column 1:1 shows the correctly delineated trees or perfect matches. About 40 reference trees were sampled in each plot, totaling 240 reference trees.

	Reference crown perspective				Delineated crown perspective						
Plot	0:1	1:1	2:1	3:1	1:0	1:1	1:2	1:3	1:1	PA[a] (%)	UA[b] (%)
A	0	35	5	0	0	38	3	0	25	63	61
B	0	30	9	1	0	32	6	0	22	55	58
C	1	29	8	3	0	48	6	2	21	51	38
D	0	31	8	1	0	40	4	0	26	65	59
E	3	30	7	0	0	28	4	0	20	50	63
F	0	26	12	2	0	32	9	1	14	35	33
All	4	181	49	7	0	218	32	3	128	53	51

[a]Producer's accuracy.
[b]User's accuracy; A = Larch; B = Sycamore; C = Oak; D = Sitka spruce; E = Norway spruce; F = Mix. A, D, and E are conifers; the others are broadleaf species.

Oak and Mix plots, predominantly with two segments (2:1 in the reference crown perspective) and not more than three segments per tree. These two plots were also the most affected by under-segmentation (1:2 and 1:3 in the delineated crown perspective). Examples of the results are shown in Fig. 5, where manual and automatic delineated polygons are overlaid on the UAV orthomosaic (all the automatic delineated crowns can be seen in Fig. 6).

As for the CHM only method, an overall accuracy of 53% and 51% was detected across all woodland types, as given by the PA and UA, respectively (Table 6). This indicates that the CHM only method produced poorer results by 10%, indicating that the inclusion of brightness data is beneficial for individual tree detection approaches. Despite such differences in magnitude, the CHM only method returned similar tendencies, with conifer species being more accurately delineated (PA = 50% to 65% and UA = 59% to 61%) than broadleaved species (PA = 35% to 55% and UA = 33% to 58%) (Table 6). Due to this overall better performance

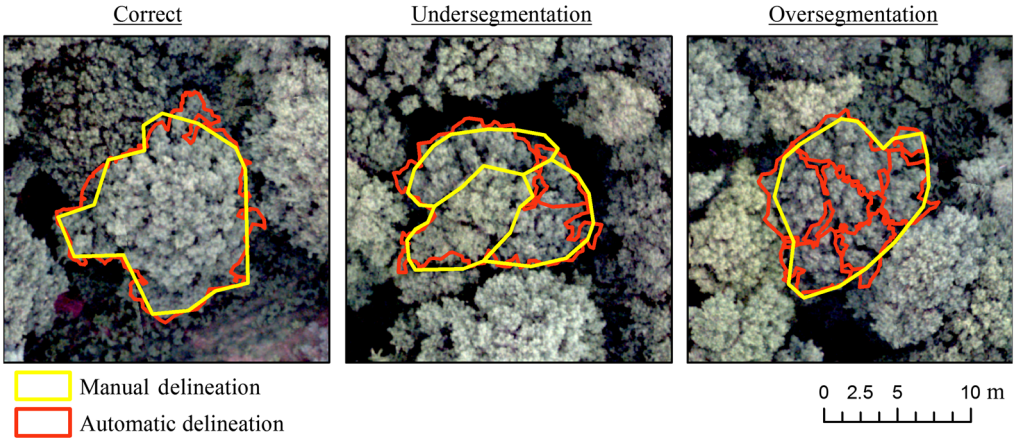

Fig. 5 Examples comparing manual versus automatic delineation of oak tree crowns for three cases: correct detection, undersegmentation, and oversegmentation. The background orthomosaic is made of visible camera UAV images, acquired on June 25, 2015.

Fig. 6 Totally 4354 tree crows were automatically detected across the study area. Orthomosaic made of RGB UAV images acquired on April 21, 2015.

of the CHM + brightness method, only the heights and crown diameters derived from this method are compared against ground measurements.

For correctly delineated crowns, crown diameters were underestimated by around 21 cm (absolute error of 42 cm and RMSE of 11%) across the six plots, with the best match occurring for the Oak plot (RMSE = 6%) and the largest mismatch for Sitka spruce (RMSE = 19%) (Table 7). This underestimation tendency means that the automatically delineated crown area is smaller than the reference crown, and this can be due to: (1) generalization of the crown shape during manual delineation, i.e., not cutting into the crown between branches when drawing crown boundaries and (2) the exclusion of areas with low brightness and low height during the automatic delineation (Fig. 2), which can favor the upper canopy.

Tree heights derived from the UAV CHM were underestimated by ~1 m (Fig. 7), with taller trees (Larch and Sycamore) contributing the most for this tendency, as indicated by the slope (<1) of the linear equation. This underestimation could be due to the spatial smoothing applied on the original CHM, as it tends to flatten the CHM surface. Generally, tree heights could be estimated from the UAV CHM with an uncertainty of ~1.5 m, as given by the RMSE value (Fig. 7).

Table 7 Summary statistics of crown diameter from correctly delineated tree crowns (perfect 1:1, Table 5, CHM + brightness method). Each plot has 40 reference tree crowns. Bias is calculated as reference less delineated crowns, so a negative bias indicates underestimation of tree crown diameter. RMSE is shown as a percentage of the mean measured diameter.[41]

Plot	Tree crowns (perfect matches)	Mean reference diameter (m)	Bias (m)	Absolute error (m)	RMSE (%)
Larch	31	5.3	−0.08	0.41	10
Sycamore	23	6.2	−0.34	0.45	9
Oak	21	7.9	−0.08	0.34	6
Sitka spruce	32	4.0	−0.47	0.57	19
Norway spruce	29	2.3	−0.18	0.26	13
Mix	17	6.3	−0.13	0.49	10
Total	153	5.3	−0.21	0.42	11

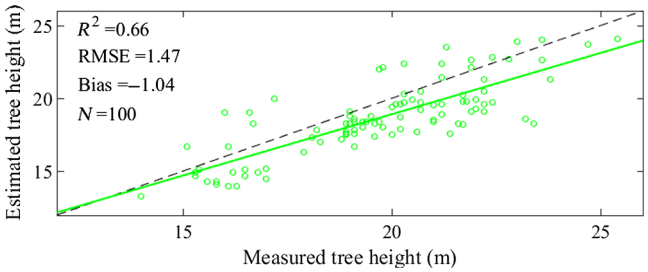

Fig. 7 Tree heights estimated from a UAV-derived CHM (CHM + brightness method) are validated against ground measured tree heights (hypsometer + transponder), across six woodland plots. The dashed line represents the 1:1 line and the solid line a linear regression model.

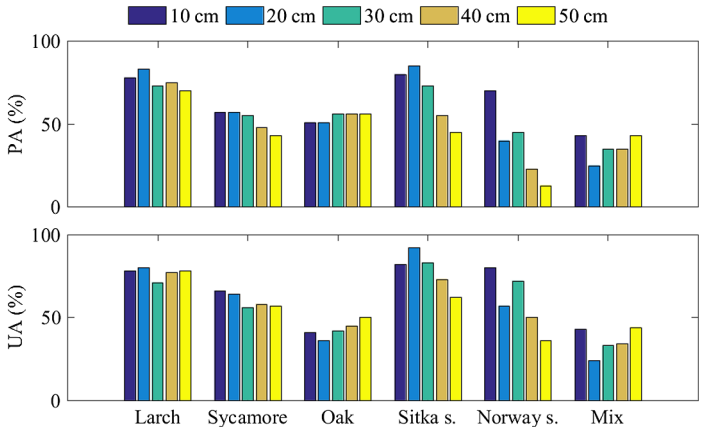

Fig. 8 Effects of spatial resolution degradation (UAV-derived CHM and orthomosaics) in the PA and UA assessment of tree crown delineation across six different test sites. About 40 reference tree crowns were considered in each test site.

Decreasing image resolution, in general, increased delineation error (Fig. 8), agreeing with Ref. 41. An exception was detected with Oak trees, which could be due to their larger crowns (diameter of ~8 m). In this case, the spatial degradation can smooth out large gaps within a tree crown, reducing oversegmentation. The highest spatial resolution data (10 cm) were therefore used for the automatic tree crown delineation.

4 Discussion

Tree crowns and tree peaks were automatically detected from high-resolution photogrammetric point clouds, alongside orthomosaic brightness information from UAV data, allowing tree crown and peaks estimation across the entire extent of the aerial survey. Combining elevation with brightness data (CHM + brightness method) improved the tree crown and tree count detection accuracy by around 10% and 5%, respectively. UAV spectral data combined with UAV point cloud data (but at the point level) were also proven to be positively influential in the accurate detection of individual trees (~6.3%) across a conifer-dominated temperate forest.[29] Because the upper canopy is usually brighter than the background cover, the brightness information showed to be particularly useful to eliminate those watershed areas and tree peak candidates not belonging to tree crowns (i.e., darkest areas), therefore improving the crown's limits detection. This is in accordance with St-Onge et al.,[15] who found that the crown outline boundaries detected from UAV photogrammetric point clouds-derived CHM tend to be less reliable (compared to Lidar) due to smoothing effects and occlusion problems. Furthermore, strong shadows, which can cause occlusions and lead to local inaccuracies in the 3-D point cloud and CHM reconstruction,[19] can be easily classified on RGB orthomosaics (e.g., Fig. 3) and used to improve crown boundary delineation.

The delineation accuracy found in this research (40% to 80%) is within the range reported in the literature for heterogeneous environments.[14,18,24,42] Similar to this work, Nuijten et al.[30] applied a watershed segmentation onto UAV-derived CHM to delineate individual tree crowns across a deciduous-dominated temperate forest, achieving accuracies between 55% and 77%, depending on the dates on which the UAV images were acquired. Yancho et al.[29] also combined spectral and point cloud UAV data (but using a subcrown point clustering approach), where 48% of the individual tree crown were correctly detected and segmented across a complex forest ecosystem. Across a boreal forest, Nevalainen et al.[19] found the accuracy of individual tree identification from the UAV photogrammetric point clouds varying between 26% and 96%, depending on the characteristics of the different test sites. These results confirm that heterogeneous forest structures (such as the Oak and Mix plots in this study) are challenging targets for automated individual tree crown detection and delineation using remotely sensed data.[21,23] On the other hand, an accuracy of >90% in delineated tree crows from UAV-derived 3-D point clouds data was reported by Torres-Sánchez et al.,[28] which is likely due to the simpler structure of the study area (an almond tree plantation).

Similarly, the uncertainties found in this study for crown diameter (absolute error of 42 cm and RMSE of 11%) and dominant height (RMSE = 1.47 m) are within the range reported in the literature for mixed, complex forest environments.[14,15] These results are similar to those achieved by St-Onge et al.,[15] who used an airborne multispectral metric camera to estimate tree height, yielding $0.53 \leq r^2 \leq 0.93$ and 1.35 m ≤ RMSE ≤ 2.4 m (depending on forest type and structure), confirming the potential of low-cost nonmetric UAV cameras for individual tree detection applications. Unlike this study, crown diameters were overestimated by ~50 cm (absolute error of ~75 cm and RMSE of ~16%) in the CHM-based method of Panagiotidis et al.,[14] which can be partially explained by the combination of pixels from gap areas being counted as crown area; this problem could potentially be minimized by applying a brightness threshold to filter out such gap areas, as proposed in this study and illustrated in Fig. 3.

Studies retrieving canopy biophysical parameters of individual trees with UAV RGB imagery across discontinuous (open) canopies achieved better results than this study, as it could be expected. Torres-Sánchez et al.[28] estimated almond tree heights with an RMSE = 0.39 m. Zarco-Tejada et al.[25] found a similar error of RMSE = 0.35 m in the estimation of tree heights across an olive orchard, using a UAV-derived digital surface model. Across a pine forest plantation, linear fits of the field and UAV image-measured height showed an $R^2 = 0.81$ (RMSE = 0.45 m), while in crown diameter an $R^2 = 0.95$ (RMSE = 0.63 m) was achieved.[16] In conifer-dominated boreal forests, Puliti et al.[17] predicted the dominant height with an accuracy of 0.7 m. These relatively good agreements are likely due to typically more simple forest types, in terms of species composition, and/or higher values of canopy gap fractions (usually sparsely distributed trees), characteristics which can make it easier for the algorithm to resolve the individual trees at both the spectral and 3-D domain.

The method may be applied to other forest areas where UAV optical data are available. The proposed workflow is based on RGB imagery from a consumer off-the-shelf digital camera onboard on a UAV, making it an affordable aerial remote sensing platform. Nevertheless, because UAV data from two acquisition dates and at an individual tree level are needed, an accurate georeferencing approach should be utilized to minimize registration errors using either GCPs surveyed with differential GPS (as in this study) or geotags from the original images (direct georeferencing) if a high accuracy GNSS receiver is available onboard the UAV; however, over areas with a high degree of canopy openness throughout the year (e.g., orchards[25]), UAV images acquired on a single date could be satisfactorily enough to reconstruct both the DTM and the DSM, as the proportions of canopy and background covers on the images are expected to be similar, reducing UAV acquisition costs and simplifying the methodology. Regarding the transferability of methodology to different forest structures (dense versus open canopies) and composition (deciduous versus conifers), different optimal parameter values within the workflow (e.g., search radius and brightness thresholds) may need to be identified and validated (sensitivity analysis).

Future studies in this research field could take advantage of the high temporal and spatial resolution of UAV imageries to iteratively improve the delineation accuracy (especially across complex forest ecosystems) by exploiting the phenological variability of individual plants growing adjacent to each other or other ecological processes such as competition among trees. Such approaches would take full advantage of the information contained within time series of remotely sensed data. Measurements of individual tree crowns that are so aptly captured in field surveys, but are lost in satellite pixel-based studies, can potentially be achieved by sensors onboard a UAV. Contrary to field surveys which have to sample an ecosystem due to costs constrains or natural limitations, the approach proposed in this study offers the chance to potentially measure all the trees in the forest upper stratum within a small area, i.e., it is possible to census the plants within this area; however, complex forest structures, such as from old broadleaved species, can make it challenging to accurately detect tree crowns, as shown here and elsewhere.[22,29,30] Bearing in mind such limitations, this approach can be extremely useful in ecological studies as it allows researchers to analyze a forest in its primary element, the tree.[5] This could be useful for many ecological applications, such as tree species or plant communities mapping,[43,44] forest phenology,[31] predicting bird phenology,[45] and can aid in understanding processes occurring at very fine scales.

4.1 *Considerations in Forest Phenology Applications*

It is commented above that one potential application of delineated tree crows is the ability to monitor the life cycle development of forests (phenology) at an individual tree level. However, consideration is needed regarding the uncertainties of this watershed-based method for individual tree-level phenology estimates more generally. Trees with multiple segments (oversegmentation) will be considered multiple trees, but the multiple segments should return very similar estimates of phenological events dates (assuming budburst occurs evenly within the same crown). On the other hand, trees clustered under one segment (undersegmentation) will be treated as a single tree and the estimated phenological events should: (1) reproduce the average behavior of the cluster, if the individuals start the growing season on similar dates or (2) if the clustered trees leaf out on very different dates, the estimated start of spring date may be more closely associated with the first tree to leaf out within the cluster.

The latter case may have implications on estimating phenological behavior at large scales. For example, if phenological event dates of such clusters are aggregated up to a moderate/coarse spatial resolution satellite pixel area, the UAV-derived canopy phenology may be biased earlier, i.e., the aggregated leaf out date will be estimated earlier in the year.

5 Conclusions

A detailed, step-by-step, watershed-based approach was proposed to automatically detect and delineate tree crowns using UAV remote sensing data (from a cheap camera) and a popular GIS

software. This can allow mapping of overstorey vegetation at a detailed biological scale and across local spatial extents and could be a useful tool for precision forestry. The proposed method can be used to detect the position, the size, and the shape of individual tree crowns from UAV-derived products (point clouds and orthomosaics).

Nevertheless, complex forest structures (due to, for example, heterogeneity in tree species composition and differences in age) are still very challenging environments to achieve accurate automatic delineation of tree crowns. Therefore, it is important to continuously test new algorithms and new remote sensing datasets to improve results, mainly over heterogeneous forests.

Acknowledgments

This work was supported by the Coordenação de Aperfeiçoamento de Pessoal de Nível Superior (CAPES) under Grant No. 1121/13-8 and by the Conselho Nacional de Desenvolvimento Científico e Tecnológico (CNPq) under Grant No. 150486/2019-7. The author would like to thank Dr. M. Peppa, Dr. M. Smigaj, and Mr. M. Robertson for their substantial help with the UAV data collection. Finally, the author would like to thank Dr. Rachel Gaulton and Dr. Stuart Barr for substantial guidance while writing this work as part of the author's PhD thesis. The author also thank the anonymous reviewers for their valuable comments and suggestions.

References

1. D. Koc-San et al., "Automatic citrus tree extraction from UAV images and digital surface models using circular Hough transform," *Comput. Electron. Agric.* **150**, 289–301 (2018).
2. X. Dong et al., "Extraction of information about individual trees from high-spatial-resolution UAV-acquired images of an orchard," *Remote Sensing* **12**(1), 133 (2020).
3. X. Yu et al., "Automatic detection of harvested trees and determination of forest growth using airborne laser scanning," *Remote Sens. Environ.* **90**(4), 451–462 (2004).
4. J. Heinzel and B. Koch, "Investigating multiple data sources for tree species classification in temperate forest and use for single tree delineation," *Int. J. Appl. Earth Obs. Geoinf.* **18**, 101–110 (2012).
5. M. Dalponte, L. Frizzera, and D. Gianelle, "Individual tree crown delineation and tree species classification with hyperspectral and LiDAR data," *PeerJ* **6**, e6227 (2019).
6. M. Dalponte et al., "Predicting stem diameters and aboveground biomass of individual trees using remote sensing data," *Ecol. Indic.* **85**, 367–376 (2018).
7. Y. Bai et al., "Quantifying tree cover in the forest–grassland ecotone of British Columbia using crown delineation and pattern detection," *For. Ecol. Manage.* **212**(1), 92–100 (2005).
8. Z. Zhen, L. J. Quackenbush, and L. Zhang, "Trends in automatic individual tree crown detection and delineation—evolution of LiDAR data," *Remote Sens.* **8**(4), 333 (2016).
9. A. O. Ok and A. Ozdarici-Ok, "2-D delineation of individual citrus trees from UAV-based dense photogrammetric surface models," *Int. J. Digit. Earth* **11**(6), 583–608 (2018).
10. D. C. Mlenek et al., "Revisão sistemática da literatura sobre detecção de árvores utilizando dados de sensoriamento remoto," *BIOFIX Sci. J.* **5**(1), 71–79 (2020).
11. J. M. A. Duncan, J. Dash, and P. M. Atkinson, "Spatio-temporal dynamics in the phenology of croplands across the Indo-Gangetic Plains," *Adv. Sp. Res.* **54**(4), 710–725 (2014).
12. C. A. Silva et al., "Imputation of individual Longleaf Pine (*Pinus palustris* Mill.) tree attributes from field and LiDAR data," *Can. J. Remote Sens.* **42**(5), 554–573 (2016).
13. F. Naveed et al., "Individual tree crown delineation using multispectral LiDAR data," *Sensors* **19**(24), 5421 (2019).
14. D. Panagiotidis et al., "Determining tree height and crown diameter from high-resolution UAV imagery," *Int. J. Remote Sens.* **38**, 2392–2410 (2017).
15. B. St-Onge, F. A. Audet, and J. Begin, "Characterizing the height structure and composition of a boreal forest using an individual tree crown approach applied to photogrammetric point clouds," *Forests* **6**(11), 3899–3922 (2015).
16. J. G. Hernandez et al., "Using high resolution UAV imagery to estimate tree variables in *Pinus pinea* plantation in Portugal," *Forest Syst.* **25**(2), eSC09 (2016).

17. S. Puliti et al., "Inventory of small forest areas using an unmanned aerial system," *Remote Sens.* **7**(8), 9632–9654 (2015).
18. Y. S. Lim et al., "Calculation of tree height and canopy crown from drone images using segmentation," *J. Korean Soc. Surv. Geod. Photogramm. Cartogr.* **33**(6), 605–614 (2015).
19. O. Nevalainen et al., "Individual tree detection and classification with UAV-based photogrammetric point clouds and hyperspectral imaging," *Remote Sens.* **9**(3), 185 (2017).
20. B. Apostol et al., "Species discrimination and individual tree detection for predicting main dendrometric characteristics in mixed temperate forests by use of airborne laser scanning and ultra-high-resolution imagery," *Sci. Total Environ.* **698**, 134074 (2020).
21. H. J. Hastings et al., "Tree species traits determine the success of LiDAR-based crown mapping in a mixed temperate forest," *Remote Sens.* **12**(2), 309 (2020).
22. Y. Ke and L. J. Quackenbush, "A comparison of three methods for automatic tree crown detection and delineation from high spatial resolution imagery," *Int. J. Remote Sens.* **32**(13), 3625–3647 (2011).
23. L. I. Duncanson et al., "An efficient, multi-layered crown delineation algorithm for mapping individual tree structure across multiple ecosystems," *Remote Sens. Environ.* **154**, 378–386 (2014).
24. D. Li et al., "Individual tree delineation in windbreaks using airborne-laser-scanning data and unmanned aerial vehicle stereo images," *IEEE Geosci. Remote Sens. Lett.* **13**(9), 1330–1334 (2016).
25. P. J. Zarco-Tejada et al., "Tree height quantification using very high resolution imagery acquired from an unmanned aerial vehicle (UAV) and automatic 3D photo-reconstruction methods," *Eur. J. Agron.* **55**, 89–99 (2014).
26. R. Kestur et al., "Tree crown detection, delineation and counting in UAV remote sensed images: a neural network based spectral–spatial method," *J. Indian Soc. Remote Sens.* **46**(6), 991–1004 (2018).
27. P. Andrade-Sanchez et al., "Development and evaluation of a field-based high-throughput phenotyping platform," *Funct. Plant Biol.* **41**, 68–79 (2014).
28. J. Torres-Sánchez et al., "Mapping the 3D structure of almond trees using UAV acquired photogrammetric point clouds and object-based image analysis," *Biosyst. Eng.* **176**, 172–184 (2018).
29. J. M. M. Yancho et al., "Fine-scale spatial and spectral clustering of UAV-acquired digital aerial photogrammetric (DAP) point clouds for individual tree crown detection and segmentation," *IEEE J. Sel. Top. Appl. Earth Obs. Remote Sens.* **12**(10), 4131–4148 (2019).
30. R. Nuijten et al., "Examining the multi-seasonal consistency of individual tree segmentation on deciduous stands using digital aerial photogrammetry (DAP) and unmanned aerial systems (UAS)," *Remote Sens.* **11**(7), 739 (2019).
31. E. F. Berra, R. Gaulton, and S. Barr, "Assessing spring phenology of a temperate woodland: a multiscale comparison of ground, unmanned aerial vehicle and Landsat satellite observations," *Remote Sens. Environ.* **223**, 229–242 (2019).
32. Newcastle University, "Cockle Park Weather Station monthly records," 2015, https://www.ncl.ac.uk/library/nclonly/cockle_park_data/.
33. L. Liang and M. D. Schwartz, "Landscape phenology: an integrative approach to seasonal vegetation dynamics," *Landsc. Ecol.* **24**(4), 465–472 (2009).
34. E. F. Berra, R. Gaulton, and S. Barr, "Commercial off-the-shelf digital cameras on unmanned aerial vehicles for multitemporal monitoring of vegetation reflectance and NDVI," *IEEE Trans. Geosci. Remote Sens.* **55**(9), 4878–4886 (2017).
35. *Agisoft PhotoScan User Manual: Professional Edition*, Version 1.2, p. 103, Agisoft LLC, St. Petersburg, Russia (2016).
36. C. Edson and M. G. Wing, "Airborne light detection and ranging (LiDAR) for individual tree stem location, height, and biomass measurements," *Remote Sens.* **3**(11), 2494 (2011).
37. C. Mei and S. Durrieu, "Tree crown delineation from digital elevation models and high resolution imagery," *Proc. IAPRS* **36**, 218–223 (2004).
38. N. A. M. Zaki et al., "Individual tree crown (ITC) delineation using watershed transformation algorithm for tropical lowland dipterocarp," in *Int. Conf. Space Sci. and Commun.*, pp. 237–242 (2015).

39. P. Axelsson, "DEM generation from laser scanner data using adaptive TIN models," *Int. Arch. Photogramm. Remote Sens.* **33**, 111–118 (2000).
40. A. Shahtahmassebi et al., "Review of shadow detection and de-shadowing methods in remote sensing," *Chin. Geogr. Sci.* **23**(4), 403–420 (2013).
41. D. A. Pouliot et al., "Automated tree crown detection and delineation in high-resolution digital camera imagery of coniferous forest regeneration," *Remote Sens. Environ.* **82**(2–3), 322–334 (2002).
42. C. Thiel and C. Schmullius, "Derivation of forest parameters from stereographic UAV data —a comparison with airborne lidar data," in *Living Planet Symp.*, L. Ouwehand, Ed., ESA-SP, Prague, Czech Republic, Vol. 740, p. 189 (2016).
43. A. Michez et al., "Classification of riparian forest species and health condition using multi-temporal and hyperspatial imagery from unmanned aerial system," *Environ. Monit. Assess.* **188**(3), 1–19 (2016).
44. J. Lisein et al., "Discrimination of deciduous tree species from time series of unmanned aerial system imagery," *PLoS One* **10**(11), e0141006 (2015).
45. E. F. Cole et al., "Predicting bird phenology from space: satellite-derived vegetation green-up signal uncovers spatial variation in phenological synchrony between birds and their environment," *Ecol. Evol.* **5**(21), 5057–5074 (2015).

Elias Fernando Berra received his BA degree in forest engineering from the Federal University of Santa Maria, Brazil, in 2010, his master's degree in remote sensing from the Federal University of Rio Grande do Sul, Brazil, in 2013, and his PhD in geospatial engineering from Newcastle University, UK, in 2018. His research interest focuses on monitoring and assessing the vegetated land surface with aid of remote sensing data and techniques.